The 'periodic nulls' of radio pulsar J1819+1305

Joanna M. Rankin[1]★ and Geoffrey A. E. Wright[2]★

[1]*Physics Department, University of Vermont, Burlington, VT 05405, USA*
[2]*Astronomy Centre, University of Sussex, Falmer BN1 9QJ*

ABSTRACT

We present a single-pulse study of the four-component pulsar J1819+1305, whose 'null' pulses bunch at periodic intervals of around 57 times the rotation period. The emission bursts between the null bunches exhibit characteristic modulations at two shorter periodicities of approximately 6.2 and 3 times the rotation period, the former found largely in the two outer components, and the latter only in the first component. Many bursts commence with bright emission in second component, exhibit positive six-period drift across the full profile width, and end with three-period modulation in the leading component. The 57-period cycle can be modelled geometrically as a sparsely filled subbeam carousel with nulls appearing whenever our line of sight intersects a circulating empty region. This interpretation is compatible with other recent evidence for periodic, carousel-related nulling and appears to support the physics of a polar-gap emission model for 'drifting' subpulses, but the subtle structure of the emission bursts defies an easy explanation.

Key words: MHD – plasmas – polarization – radiation mechanisms: non-thermal – methods: data analysis – pulsars: individual: J1819+1305.

1 INTRODUCTION

Pulsar J1819+1305 was discovered twice, once in a Swinbourne survey (Edwards et al. 2001) and also in the Arecibo 430-MHz survey of Navarro, Anderson & Freire (2003, hereafter NAF). The latter paper notes that this pulsar is the brightest of the nine stars discovered, and using pulse-sequence (hereafter PS) observations they were able to identify several of its outstanding characteristics. First among these is the star's tendency to 'null' roughly half of the time, a feature not uncommon in pulsars with a large spin-down age (47 Myr for J1819+1305). However, a second very strange circumstance is that the observed 'null' intervals exhibited a strong periodicity of 53 ± 3 times the rotation period (hereafter P_1) of 1.06 s. A 1000-period section of their observation is shown in their fig. 6, and some 18 nearly equally spaced bursts of emission are clearly evident. The figure also shows the star's asymmetric, apparently triple, profile and the text notes that a part of the intensity variation is due to 'strong intensity modulation of the first component'.

The J1819+1305 section of the NAF paper remarks that little further analysis could be made without polarimetry and thus an understanding of the pulsar's emission geometry, but that, were this available, 'a proper interpretation of the nulling might lead to new insights'. We have observed the pulsar a number of times with the intention of studying its periodic nulling behaviour. Our observations are described in Section 2, and Section 3 assesses the star's

fundamental emission geometry. Section 4 presents our analysis of the 'nulls' and their periodicity and Section 5 analyses the modulation of the emission bursts. In Section 6 we interpret the null periodicity as a 'carousel' circulation time and give examples of the often incomplete patterns which can reproduce the pulsar's observed behaviour. Section 7 summarizes and discusses our results.

2 OBSERVATIONS

The observations used in our analyses were made using the 305-m Arecibo Telescope in Puerto Rico. The 327-MHz (*P* band) and 1400-MHz (*L* band) polarized PSs were acquired using the upgraded instrument together with the Wideband Arecibo Pulsar Processor (WAPP[1]) over the last three years. The auto-correlation and cross-correlations of the channel voltages produced by receivers connected to orthogonal linearly polarized feeds (circular after 2004 October 11) were three-level sampled. Upon Fourier transforming, sufficient channels were synthesized across a 25-MHz (100-MHz at *L* band) bandpass to provide resolutions of some 1 milliperiod of longitude. The Stokes parameters have been corrected for dispersion, interstellar Faraday rotation,[2] and various instrumental polarization effects. At *L* band, four 100-MHz channels were observed with centres at 1170, 1420, 1520 and 1620 MHz. Some of the observations encountered virtually no interference (hereafter RFI); others, however, were

---

★E-mail: joanna.rankin@uvm.edu (JMR); g.wright@sussex.ac.uk (GAEW)

[1] http://www.naic.edu/~wapp.
[2] The star's rotation measure was measured as $+119 \pm 4$ rad m^2.

rendered useless for some analytical purposes by radar and other RFI sources. We were able to largely clean the several brief RFI events from the MJD 53778 observation, but for two others (MJDs 52941 and 53859) this has not been fully possible; see Table 1.

3 EMISSION GEOMETRY

The needed polarization profile of J1819+1305 is given in Fig. 1, and here we again see the star's asymmetric three-component profile. Both recent *P*-band observations exhibit nearly identical such profiles, and those at *L* band are also quite similar, apart from being more compact and having a somewhat more intense trailing 'component'. The profiles from both bands show the prominent, positive-going polarization angle (hereafter PA) traverse with a central slope *R* of about +7° per degree.

Overall, the profile appears entirely conal, and the linear polarization shows evidence of a fourth component which is echoed by inflections in the total power. Longitude–longitude correlation maps at zero delay (not shown) exhibit a roughly symmetrical form with distinct regions of self-correlation near ±10° and a third broad area between some ±7°. The conal character of J1819+1305's emission is supported by its small value of B_{12}/P_1^2 (where B_{12} is the surface magnetic field in units of 10^{12} G) of 0.6, reflecting its nearly 1-s P_1 and small spin-down. This interpretation makes the pulsar a rare member of the conal quadruple (cQ) class (e.g. see Rankin 1993a,b, hereafter Paper V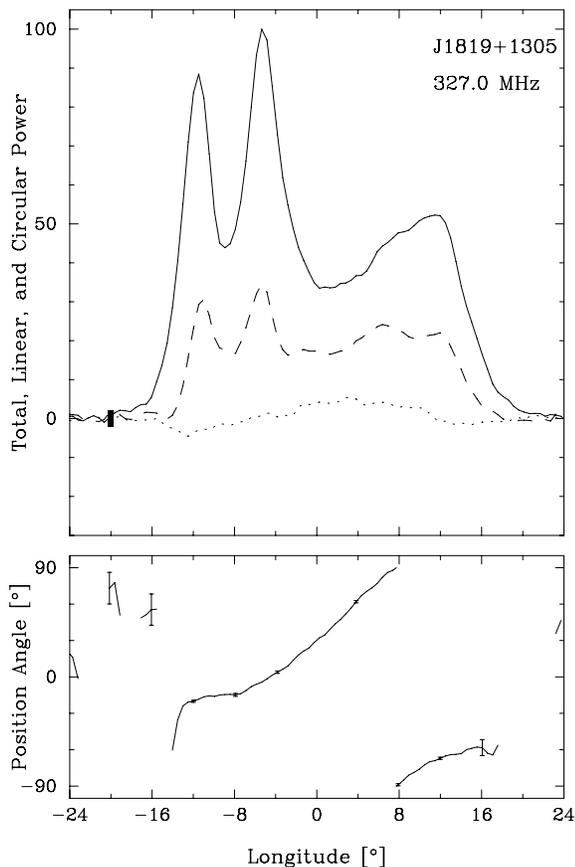I), where our sightline cuts two concentric emis-sion cones but fails to encounter appreciable core radiation. Note also the pronounced edge depolarization, which is a reliable de-markation of the outer conal edge (Rankin & Ramachandran 2003) due to the presence of both orthogonal polarization modes at roughly equal intensity. The pulsar is too weak for these to be seen in individual pulses, but each of our average profiles gives evidence of the '90° jumps' on one or both edges that they often produce. It is interesting to compare J1819+1305's profile with that of the long known B1918+19 (i.e. Hankins & Wolszczan 1987; Brown et al. 2008) which has a similar sightline geometry and thus profile, but a conal triple form. In both cases the trailing half of the profile is attenuated, perhaps a result of 'absorption'.

On this basis it is straightforward to work out the star's basic geometry. The *P*- and *L*-band profiles have outside half-power widths of some 28° and 23°, respectively, providing a decent estimate of its 1-GHz width $\Delta\Psi$ of 24°. Then following the procedures of Paper VI, J1819+1305's magnetic latitude α and sightline-impact angle β can be computed from *R* and $\Delta\Psi$ to be some 22° and +3°.0, respectively – making β/ρ 0.53 for the outer cone, where ρ is the emission-cone radius to the outside half-power point. Moreover, the roughly 15° outside, half-power width of the inner conal component pair squares well with this value of α. Given he clear flattening of the PA traverse at the profile edges, we take the sign of β to be positive.

4 ANALYSIS

4.1 The null and emission distribution

Although B1819+1305 is reasonably strong at 327 MHz, its null histogram in Fig. 2 shows that its nulls and weak pulses cannot be fully distinguished, if indeed they are distinguishable at all. The pulse-intensity distribution is sufficiently broad that some apparently null pulses may simply correspond to pulses in the weak tail of the distribution. Only the large secondary distribution around zero indicates that there is a distinct population of ostensibly 'true' nulls whose intrinsic properties make them indistinguishable from weak normal pulses.

In order to proceed, we took a conservative definition of the intensity boundary between the pulses and 'nulls', 0.29 $\langle I \rangle$, shown by

Figure 1. Integrated profile of 3394 pulses from J1819+1305 at 327 MHz. The top panel shows the total intensity (Stokes *I*; solid curve), the total linear (Stokes *L*; dashed) and the circular polarization (Stokes *V*; dotted). The lower panel shows the average PA traverse.
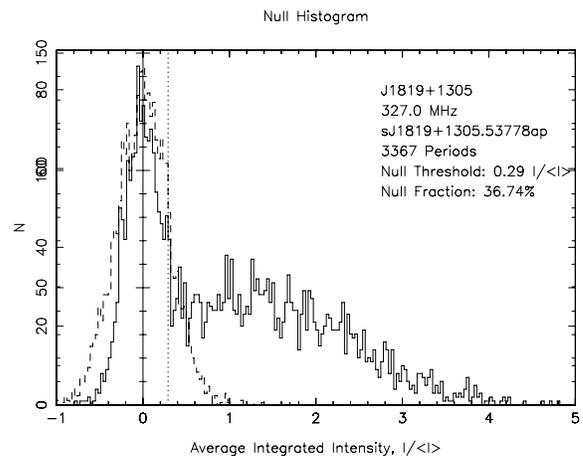

Figure 2. Null histogram corresponding to the long 327-MHz observation of MJD 53778 (as in Fig. 1). The solid and dashed curves represent the pulse and off-pulse regions, respectively. The pulse- and null-intensity distributions clearly overlap, and the vertical dotted line at 0.29 $\langle I \rangle$ shows an arbitrary, but conservative boundary between the two populations. On this basis, some 39 per cent of B1819+1305's pulses are 'nulls'.
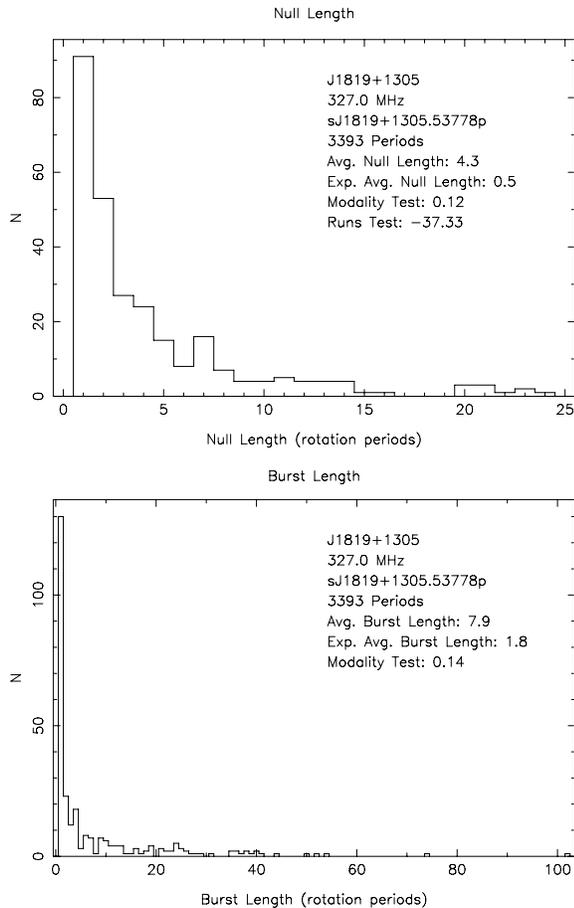
Null Length

J1819+1305
327.0 MHz
sJ1819+1305.53778p
3393 Periods
Avg. Null Length: 4.3
Exp. Avg. Null Length: 0.5
Modality Test: 0.12
Runs Test: −37.33

Burst Length

J1819+1305
327.0 MHz
sJ1819+1305.53778p
3393 Periods
Avg. Burst Length: 7.9
Exp. Avg. Burst Length: 1.8
Modality Test: 0.14

Figure 3. 'Null' and burst length distributions computed from the same PS as in Figs 1 and 2. Both burst and 'null' lengths of 1 P_1 appear to be favoured, and in both cases the mean lengths are 5–10 P_1. Significantly, however, the maximum duration of both the bursts and 'nulls' seems to be around 50 P_1.

a vertical dotted line in the histogram. On this basis, some one-third of the pulses are 'nulls'. We then identified the lengths of contiguous 'nulls' and 'bursts' in our 3392-length PS at 327 MHz on MJD 53778, and the resulting distributions are shown in Fig. 3. In the upper panel we see the null-length distribution apparently dominated by the 90 1-period nulls, a total which statistically declines to just 4 for 10-period nulls in a manner roughly conforming with a random distribution among the non-null pulses. However, this distribution comprises only 780 or two-thirds of all the 'nulls', still leaving some 420 non-random 'nulls' which are contained in sequences of 10 periods or more: note the cluster of 10 null sequences with lengths between 20 and 24 P_1. A consistent interpretation of this result would be to view the short 'nulls' as predominantly weak normal pulses falling randomly within the emission bursts, with the ostensible 'true' nulls occurring in clusters of 10 or more. Allowing for an overlap between these distributions, one may therefore estimate that no more than about 10 per cent (1/3 of 1/3) of all pulses in J1819+1305 could be 'true' nulls.[3]

In the burst length distribution (Fig. 3, lower panel), the total of 130 single-pulses preceded and followed by a null may seem high, but in fact this is well below what would be expected from a ran-

dom distribution of nulls with 1/3 chance among non-null pulses with a 2/3 probability. This expectation would be approximately $(0.33)^2 \times 0.66 \times 3392 = 250$ pulses. To obtain the observed distribution, the chance of a null occurring before or after a non-null pulse must be closer to 1/4, and for a two-pulse burst just 10 per cent, reflecting the observed non-random bunching of the non-null pulses. The implication is that the probability of a null after a null or series of nulls must be considerably higher than 1/3, thus encouraging the formation of long ($>10\,P_1$) nulls which comprise the 'periodic' null bunches. However, as with the null histogram, note that some very long emission sequences are observed – two over about 75 and four between 40 and 60 periods – showing that the apparent periodicity of the null bunches is not a precise rhythm.

4.2 The slow ($\approx 50\,P_1$) modulation

As reported by NAF, pulsar J1819+1305 exhibits the peculiar property of 'periodic nulls', and Fig. 4 gives a plot of pulse intensity versus number which dramatically illustrates this strange phenomenon. Closer inspection, however, shows irregularities in the 'null' spacings, and at several points the emission persists for up to about 100 pulses. Each of our PSs exhibits very strong 'null' modulation with a period of about 50 P_1, but of all our observations this MJD 53378 PS is the most regular. Thus, it would seem that NAF's 1000-pulse observation was unusually periodic.

Even more striking, perhaps, are the fluctuation spectra computed from the pulsar's PSs. The longitude-resolved fluctuation (hereafter LRF) spectra in Fig. 5, in this case corresponding to the long MJD 53778 observation, are typical of those resulting from our several observations. All exhibit a primary fluctuation feature at roughly 0.017 cycles/P_1 (hereafter c/P_1), corresponding to a period between 50 and 60 P_1, which is seen across the full width of the profile. All of the harmonic resolved fluctuation (hereafter HRF) spectra have a structure like that of Fig. 6 – that is, a pair of features at positive and negative frequencies of which the former is dominant. A number of higher frequency features are also visible in Figs 5 and 6 that will be further discussed in the next section.

Accurate measurements of the low-frequency modulation features were attempted across all our observations, and the results are summarized in Table 2. In each case we used an HRF of length 256, and then examined the structure of the stronger (positive)
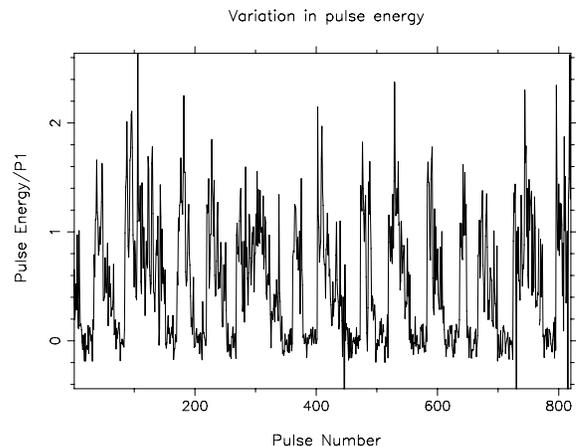

Variation in pulse energy

Figure 4. Total intensity versus pulse number for the 327-MHz PS of MJD 53378. Note the 'periodic nulls' which though not fully regular are more nearly so in this PS than others. The last part of the PS was corrupted by RFI (as are the negative deflections near pulses 440 and 725) and so is omitted.

---

[3] The RUNS test result in the figure also indicates that the nulls are greatly overclustered; see Redman & Rankin (in preparation).
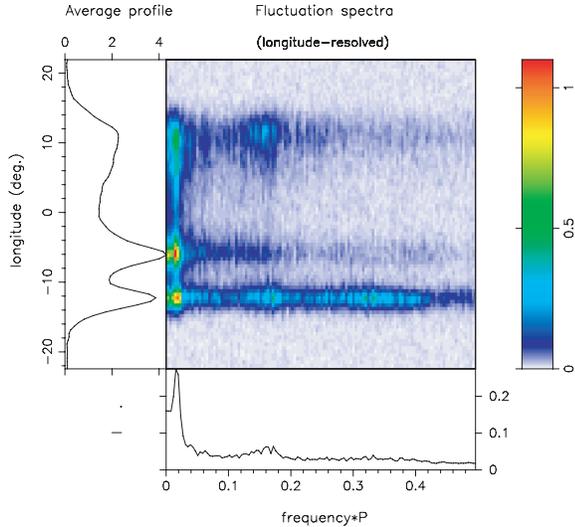
Figure 5. LRF spectra of the 3394 pulses in the MJD 53778 observation. The prominent 50 P_1 feature is the dominant response in each of our PSs and is seen over the full width of the profile. However, features corresponding to P_3 values of $\approx 6.2\,P_1$ are prominent in the outer components, and evidence of weak $P_3 \approx 3\,P_1$ modulation is exclusively present in the leading component. A 256-length FFT was used to produce these spectra.
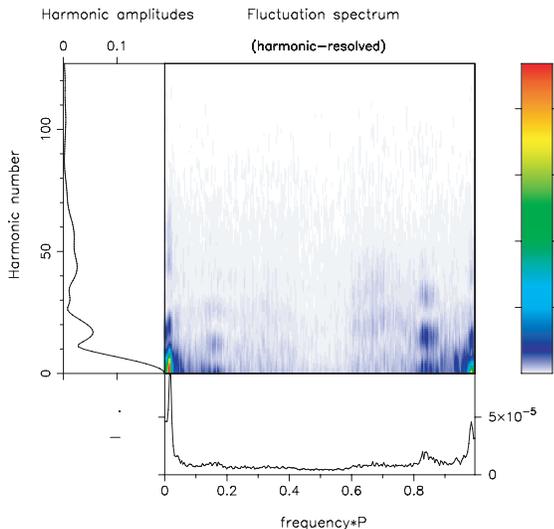

Figure 6. HRF spectrum corresponding to the same PS as in Fig. 5. Both the positive and negative frequency components corresponding to the 50 P_1 feature are evident, and the amplitude difference suggests that it represents a combination of amplitude and a phase modulation corresponding to 'drift' from trailing-to-leading regions of the profile. By contrast, the asymmetric power at about 0.85 P_1 suggests leading-to-trailing 'drift' of the 6.2 P_1 modulations seen in the spectrum of Fig. 5.

feature at about 0.017 c/P_1. Two of our observations were sufficiently corrupted by RFI that no reliable determination could be made. In the others the primary features comprised significant power in two Fourier components with periods of 51.2 and 64.0 P_1, and the tabulated values represent an appropriate weighting of their amplitudes. Remarkably, the three reliable determinations yield compatible values of about 57 ± 1 P_1. The large error reflects the limited facility of fluctuation spectra to determine the period of such a

Table 1. Arecibo single-pulse polarimetry observations.

Band	MJD Date	Channels	Resolution (°)	Pulses RFI
P	52707[a] 2003 March 10	128	0.35	1697 Clean
P	52941 2003 October 29	256	0.17	955 Bad
P	53378 2005 January 8	512	0.44	848 Good
P	53778 2006 February 12	256	0.51	3394 Clean
L	53859 2006 May 4	64	0.35	2075 Poor

[a]Unfortunately, an error in the WAPP software resulted in only one linear polarization being recorded, fourfold redundant, during the initial 2003 March session.

Table 2. PS modulation properties.

Band	MJD	Modulation period	Pulses
P	52707	56.9. ± 1.0	1697
P	52941	–	955
P	53378	57.3. ± 1.0	848
P	53778	57.0. ± 1.0	3394
L	53859	–	2075

lengthy modulation cycle. We can also probably understand how it was that NAF understood the nulls to have a roughly 50 P_1 period.

That the star's 'periodic nulls' give rise to such a well-defined low-frequency modulation feature is itself a perplexing property. They can be regarded, however, in a Fourier sense, as negative power. Apparently, we must thus conclude that the star's emission is strongly modulated with a period of about 57 P_1 – and most significantly that this is so *in spite of* the obvious irregularities in the observed PSs (there evidently can be uninterrupted emission of up to 130 pulses, as in Fig. 7).

5 THE EMISSION STRUCTURE OF THE BURSTS

We have established a picture of J1819+1305 as one of a series of emission bursts regularly punctuated by lengthy nulls. However, on inspection, the bursts themselves are found to exhibit characteristic emission patterns which are already hinted at by short-term features in the spectra of Figs 5 and 6. These features are found in all our observations, and are evidently not smeared out by long integrations. In Fig. 5 the two most obvious are the peaks corresponding to the periodicities of 6.2 P_1 and 3 P_1. The former is shared by the two outer components, suggesting a conal link, but the latter is confined to the first component. There is only weak evidence that the two inner components, presumably corresponding to a sightline intersection across an inner cone, show any regular short-term modulation. The HRF spectrum in Fig. 6, having power corresponding to the two short-term features in its second half, indicates that these arise from positive drift (i.e. from leading to trailing longitudes), in contrast to the opposite weighting for the long-term modulation generated by the nulls.

Close inspection of the PSs reveals how these features interact in a two-pattern process. Fig. 4 shows a series of typical bursts in the MJD 53378 observation, which can vary in length from 20 to
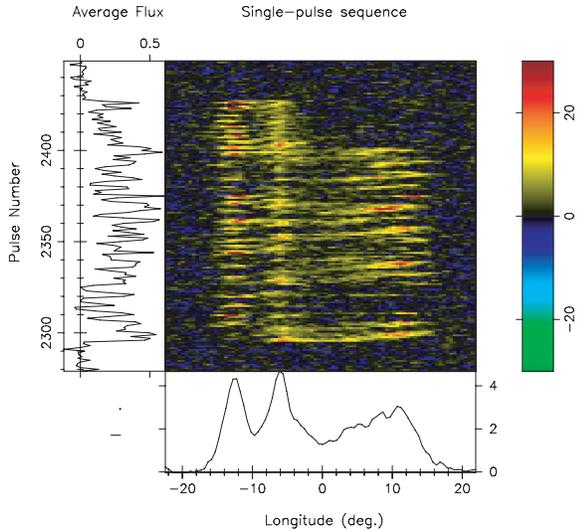
Average Flux   Single-pulse sequence

Figure 7. Display of pulses 2281–2450 extracted from the MJD 53778 observation. The PS is unusual in that it is not interrupted by nulls and also illustrates the character of both the 6.2 and 3 P_1 modulations. Note that the 6 P_1 pattern is retained in the trailing region after the 3 $P_1 P_3$ intermittently appears in the first component at about pulse 2340. Note also the characteristic disappearance of the trailing components when the 3 P_1 pattern becomes dominant in the first component after about pulse 2405.

130 pulses, and an exceptionally long burst from the MJD 53778 PS is plotted in detail in Fig. 7. Most bursts, of whatever length, commence with emission in several components (always including 2), and the 6.2 P_1 modulation is very evident as a clear positive drift in either or both of the outer components. Then, after a number of 6.2 P_1 cycles, this modulation is rapidly transformed into a shorter sequence with the 3 P_1 modulation evident in the first component only. In this second pattern, the third and fourth components are no longer detectable (e.g. after about pulse 2405 in Fig. 7). The 3 P_1 cycles are typically (but not invariably) repeated about the same number of times as the preceding longer cycles, so that this second behaviour lasts for less than half the duration of the first, before all emission ceases and the pulsar enters a null phase which may last for anything between 10 and 40 rotation periods. Short integrations over the two patterns of the bursts show that the initial phase has a broad four-peak intensity profile with no component dominating the others, whereas the second phase has just two sharp leading peaks. Clearly, the overall profile in Fig. 1 arises from the addition of these two modulation-pattern profiles.

It can also be seen from Fig. 7 that the lack of emission in the latter part of the profile in the second burst pattern gives an overall intensity 'drift' behaviour from trailing-to-leading longitudes over the burst as a whole. This is almost certainly the origin of the apparent asymmetry in the paired low-frequency features evident in the HRF of Fig. 6.

The 6.2 P_1 periodicity may occur in either or both of the outer components. When the modulation is evident in both components there appears (by eye) to be a consistent delay of approximately 2 P_1 by which the trailing component's intensity follows that of the leading, but there is no evidence of drift bands linking the components right across the profile. However, in each of the outer components short positively drifting bands can be seen. In the leading components the drift slows as the longitude of the second component is reached, a feature which is even more marked during the 3 P_1 modulation: often the drift clearly becomes stationary at the sec-

ond component, which therefore shows no significant modulation periodicity (Fig. 5). On those occasions when a drift band is clearly evident, especially in the trailing components, the drift rate is slow. If the drift were projected to match the modulated intensity peaks on the opposing outer components, drift bands would take about 8 P_1 to move across the full profile.

It should be noted that there are frequent variations on this basic two-pattern picture of the emission bursts. Sometimes one or other of the patterns is unusually long compared to the other. Occasionally, the first pattern restarts rapidly after the second without an intervening long null sequence, leading to an unusually long emission burst. The 3 P_1 modulation can seem sometimes to commence while the 6 P_1 modulation persists in the trailing components (as in Fig. 7 from about pulse 2340). Nevertheless, there appears to be a 'rule', which must have some physical significance, that the 6.2 P_1 modulation is generally followed by the faster modulation, and not the reverse. In this respect, J1819+1305 has much in common with B0031−07, B2319+60 and B1918+19, which also have 'quantized' subpulse drift rates governed by succession rules (see Wright & Fowler 1981; Wright & Fowler 1982 and Hankins & Wolszczan 1987, respectively)

6 MODELLING THE NULL–BURST CYCLE

Two basic properties of J1819+1305's subpulse behaviour have been established. First, and primarily, that the null pulses tend to bunch together and that these bunches occur on a quasi-periodic basis. Secondly, that the intervening bursts of emission have two characteristic patterns such that a 6.2 P_1 modulation in the outer components is usually followed by a 3 P_1 modulation present in the first component only.

Both these features suggest the idea of an underlying cycle regularly repeating itself, with secular modulations superimposed on the cycle so that no two cycles are the same. A natural model which would support these properties is that of the 'carousel', whereby a pattern of 'beamlets' are carried around the pulsar's magnetic axis close to its surface and are randomly sampled by the observer's line of sight. Such a carousel with, say, 70 per cent of its beamlets persistent and active would indeed generate a modulation feature reflecting its circulation time, as observed. Whether or not one accepts the physical basis of this model (and it has been modified considerably over the years – e.g. Ruderman & Sutherland 1975; Wright 2003; Gil, Melikidze & Zhang 2006), in the present context its geometry is a convenient and dynamic way of modelling the observed cyclic patterns.

In the carousel picture one naturally interprets the repetition time of the cycle as a circulation time. This implies that the recurrent bunches of nulls are seen as regions of 'empty' emission convected around the pole. It is then of interest to see how the observed emission bursts, with their dual modulation patterns and double cone structure, would appear in such a geometry. We have therefore constructed visual images of the conjectured carousel – 'polar maps' – using the cartographic transform of Deshpande & Rankin (2001) – using the underlying geometry of the star, derived in Section 3, and assuming the mean circulation time of 57 P_1 derived in Section 4. The sense of the drift is taken as positive since this is the sense found in both the first and fourth components during the emission bursts.

6.1 Polar emission patterns

We have computed polar emission maps and movies corresponding to the several available PSs, and two are shown in Fig. 8. The
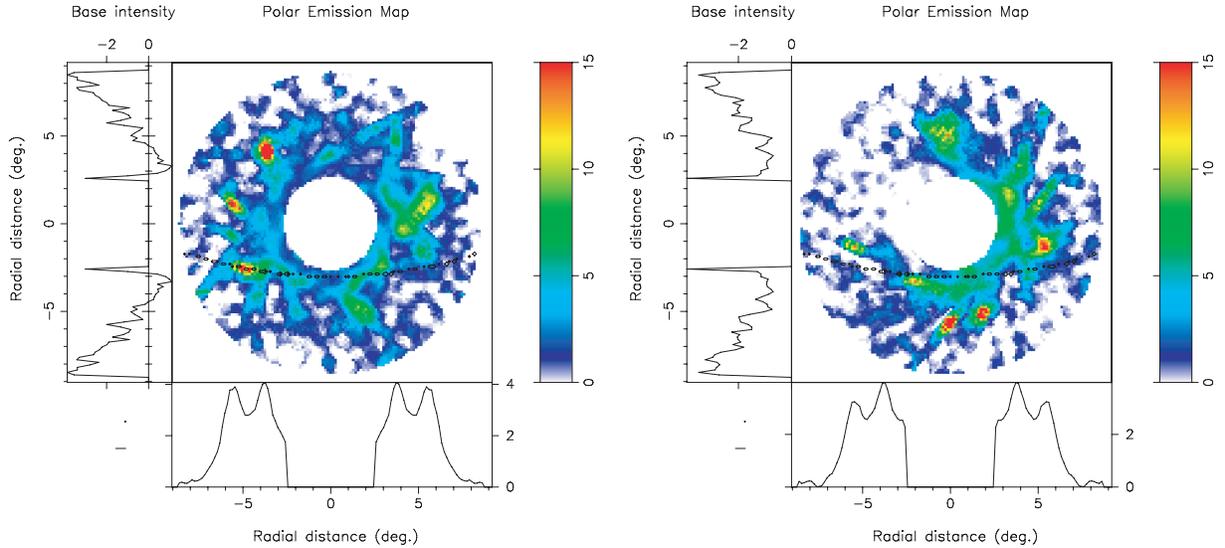
Figure 8. Subbeam 'carousel' maps (central panels) of the MJD 53778 observation produced using the cartographic mapping methods described in Deshpande & Rankin (2001). Each comprises 57 pulses, the sequence beginning at pulse 271 (left-hand part) has few 'nulls' whereas that starting at pulse 2053 (right-hand part) includes a long 'null' interval. The bottom panels give the radial emission profile and the side panels the unmodulated 'base' (which has not been subtracted from the central emission patterns). The sightline paths are shown in contours for an (assumed) outer traverse.

left-hand display gives a polar map corresponding to an interval with relatively few 'nulls', whereas about half the pulses in the right-hand PS are 'nulls'. We note that these maps correspond to only a single 57 P_1 circulation time, so they are necessarily more poorly sampled that those computed for stars with stable carousel configurations. There is no evidence that most of the 'beamlets' encountered are active even over this short interval. Indeed, when 'movies' consisting of multiple successive frames like these are viewed together, we see little evidence that particular 'beamlets' persist for a full circulation. One can see instances in each map where the sightline traverses a given 'beamlet' at several different angles, indicating that it persisted long enough to be tracked through both of the two outer cone components. And other passes can be seen where only weak noise-like emission was encountered. Also, we can see again here the double-cone structure of the map (and radial beamform in the lower panels) compatible with the emission geometry worked out in Section 3.

Fig. 9 gives a map corresponding to that part of the long burst of Fig. 7 where emission is seen across the entire profile (pulses 2296–2402). Here we see a few fairly regularly spaced 'beamlets' which seem to produce the bright 6.2 P_1 LRF feature. Note that these 'beamlets' are primarily seen in the outer conal region – and the feature is most prominent at these longitudes in the LRF – though there appears to be a weaker system in the inner cone as well. Note also that a similar 'beamlet' pattern is seen in the sub-PS of Fig. 8 (left-hand part), and a closer inspection indicates that some of these 'beamlets' do persist for a couple of circulation times at this point in the overall PS, perhaps explaining why the drift feature is more prominent here. Finally, we have made 'movies' consisting of multiple frames like those seen above.[4]

We do not understand why it is that some pulsars exhibit a double conal emission configuration, nor indeed why most all conal
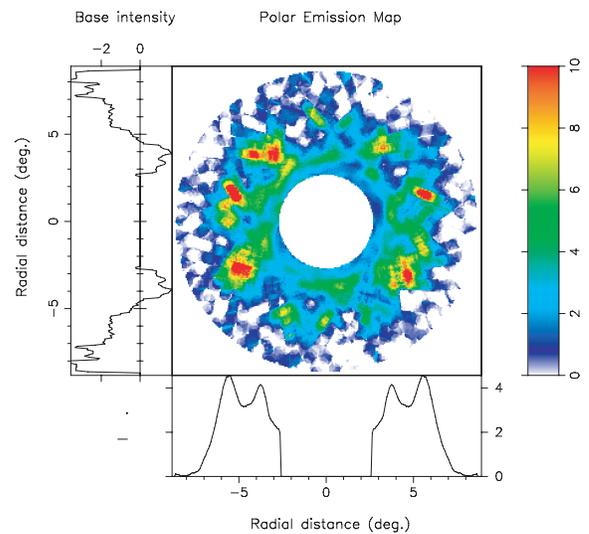

Figure 9. Polar map as in Fig. 8 for the pulse 2296–2402 interval taken from the MJD 53778 observation displayed in Fig. 7. This 'average' map shows the subbeam-carousel structure responsible for the apparent subpulse drift with a P_3 of about 6.2 P_1.

emission has an either outer or inner conal geometry. J1819+1305 and other pulsars with a similar configuration provide opportunity to examine the dynamics of the emission in the two cones. That every measurable aspect of the 'beamlet' structure in the two cones exhibits the same circulation time, drift direction, and P_3 strongly suggests that the emission within the respective cones is produced by the same set of emitting particles.

7 SUMMARY OF RESULTS AND DISCUSSION

J1819+1305 exhibits an asymmetrical profile (Fig. 1) over a broad-band which appears to reflect emission from both the outer

---

[4] These can be downloaded and/or viewed by accessing www.uvm.edu/jmrankin under the 'Research/Images & Movies' menus.

and inner emission cones. Thus we have classified it as having a cQ profile despite the difficulty of distinguishing the trailing components in its profiles. Profile polarimetry permits us to estimate the star's magnetic latitude α and sightline impact angle β as about $32°$ and $3°\!.0$, respectively. β/ρ should then be some 0.53. Though we have assumed an equatorward (positive) sightline traverse, no strong evidence exists to determine the sign of β.

The PSs of pulsar J1819+1305 were already known (NAF) to exhibit 'periodic nulls', in which the pulsar's emission appears to switch on and off for several rotation periods with a fairly regular 50-rotation-period cycle. Our fluctuation spectra over multiple observations reveal that the star's PSs indeed regularly exhibit a bright and narrow low-frequency feature. This striking feature permits relatively accurate measurement and is found to represent a $57 \pm 1\,P_1$ period in each observation – very nearly the same interval as seen qualitatively in the 'periodic nulls'. Its positive and negative components show that it has both an amplitude and a phase-modulation character, reflecting the characteristic patterns formed by the emission bursts which occur between the null bunches.

Other than their periodicity, nothing about the 'nulls' themselves appears extraordinary. An analysis shows immediately that the populations of weak pulses and 'true' nulls cannot be fully distinguished (Fig. 2). However, a careful analysis of null and burst lengths clarified the situation: while short nulls occurred randomly (as would typical weak pulses), longer nulls (>10 periods) – corresponding to the periodic bunches of 'true' nulls – were overabundant, suggesting some underlying structural feature.

On examining the emission bursts between the null bunches we noted clear examples of subpulse drift towards increasing longitude (positive) at both the 6.2 and $3\,P_1$ periodicities. The interaction of these two drift patterns is subtle. The drift bands at the repetition rate of $6.2\,P_1$ traverse both the leading and trailing components. By contrast, those of $3\,P_1$ are confined to the first components and are always accompanied by strong emission in the second component together with a striking lack of emission in the third and fourth components. Furthermore, the $6\,P_1$ pattern always precedes $3\,P_1$ intervals, although the $3\,P_1$ modulation sometimes begins before the $6\,P_1$ pattern expires. Thus the pulsar's irregular aggregate profile is a combination of a regular four-peaked profile arising from the $6\,P_1$ modulation and the sharp two-component profile of the $3\,P_1$ modulation. The fact that there is a sequence rule between the two patterns in each burst, and therefore that emission in the trailing half of the profile ceases before that in the first naturally explains why the low-frequency feature in the spectra suggests a long-term phase modulation towards the leading component. It also accounts for an observed strong anticorrelation between the leading and trailing components at a delay of around $22\,P_1$ – approximately half the burst length.

J1819+1305's regular cycle of alternating long nulls and emission bursts can be modelled geometrically as a rotating carousel with the $57\,P_1$ modulation reflecting the carousel circulation time $\hat{P}_3$, and the 'nulls' representing sightline passes through the carousel which fail to encounter significant emission. This model therefore does not require nulls to correspond to a complete cessation of emission throughout the magnetosphere, merely that 'empty' regions of the carousel circulate and maintain their identity for significantly longer than $\hat{P}_3$, giving rise to a large and obvious population of pseudo-nulls. We have argued earlier (Rankin & Wright 2007) that the much smaller proportion of 'nulls' in the Cambridge pulsar B0834+06 are also pseudo-nulls, and this second type of ostensible null may be more common that heretofore realized. Herfindal & Rankin (2007, 2008), moreover, have identified null periodici-

ties in Cambridge pulsar B1133+16 and several other stars. Can it be, for instance, that the nulls in pulsars B1918+19 (Hankins & Wolszczan 1987) and B1944+17 (Deich et al. 1986) are also of this character?

The carousel model, though here in essence no more than a geometric representation of the observed emission cycle, had its physical genesis in the work of Ruderman & Sutherland's polar gap theory (1975). In this respect it encounters difficulty. First, B1819+1305's $\hat{P}_3$ value of $57\,P_1$ is very long compared to that expected in polar gap theory. For a very usual pulsar with a 1.06-s P_1 and 6.3×10^{11} G field, it would predict a value of barely $4\,P_1$. Even if this star behaved as does B0943+10 (Deshpande & Rankin 2001) – also with a longer value than predicted by the above theory – its $\hat{P}_3$ would be some $12.6\,P_1$. Thus to account for the much slower observed drift rate a reduced electric potential across the gap [as in the theoretical modifications suggested by Harding, Muslimov & Zhang (2002) or Gil et al. (2006)] may be needed.

Another perplexing difficulty results from the subtle behaviour of the internull emission within the cycle. This shows two distinct drift modes, one about twice the repetition rate of the other. Where this occurs in other pulsars (e.g. B0031−07, B2303+30, etc.), it is easy to postulate that the circulation has, for some unknown reason, speeded up the very same 'beamlets' (e.g. Redman, Wright & Rankin 2005). This is harder to allege for J1819+1305 because it would be in conflict with the ostensible regular carousel circulation rate. We would have to reason that certain sectors of the carousel were twice as densely populated by 'beamlets' than others, although this would not obviously explain why we tend to see the former immediately after the other. Furthermore, the fact that the more rapid modulation at $3\,P_1$ is confined to the first component of the profile and generally accompanied by the 'nulling' of the third and fourth components appears to coordinate two different sections of the underlying double cone, related only by the chance intersection of our line of sight. One possibility is that the $3\,P_1$ modulation reflects a pattern of orthogonally polarized modal beamlets (as per Rankin & Ramachandran 2003), but we have not been able to confirm this circumstance owing to the weakness of the pulsar's PS emission. However, this cannot easily explain why the $3\,P_1$ modulation is *never* found in the trailing components.

ACKNOWLEDGMENTS

REFERENCES

Brown A., Rankin J. M., Wright G. A. E., 2008, MNRAS, submitted
Deich W. T. S., Cordes J. M., Hankins T. H., Rankin J. M., 1986, MNRAS, 300, 540
Deshpande A. A., Rankin J. M., 2001, MNRAS, 322, 438
Edwards R. T., Bailes M., van Stratten W., Britton M. C., 2001, MNRAS, 326, 358
Gil J., Melikidze G., Zhang B., 2006, A&A, 457, L5
Hankins T. H., Wolszczan A., 1987, ApJ, 318, 410
Harding A. K., Muslimov A., Zhang B., 2002, ApJ, 576, 366

Herfindal J., Rankin J. M., 2007, MNRAS, 380, 430
Herfindal J., Rankin J. M., 2008, MNRAS, in press
Navarro J., Anderson S. B., Freire P. C., 2003, ApJ, 594, 943 (NAF)
Rankin J. M., 1986, ApJ, 301, 901
Rankin J. M., 1993a, ApJ, 405, 285
Rankin J. M., 1993b, ApJS, 85, 145 (Paper VI)
Rankin J. M., Ramachandran R., 2003, ApJ, 590, 411

Rankin J. M., Wright G. A. E., 2007, MNRAS, 590, 411
Redman S. R., Wright G. A. E., Rankin J. M., 2005, MNRAS, 375, 859
Ruderman M., Sutherland P., 1975, ApJ, 196, 51
Wright G. A. E., 2003, MNRAS, 379, 507

This paper has been typeset from a TEX/LATEX file prepared by the author.